Notch2 (but not Notch1) is required for proximal fate acquisition in the mammalian nephron

Hui-Teng Cheng[1], **Mijin Kim**[1], **M Todd Valerius**[2], **Kameswaran Surendran**[1], **Karin Schuster-Gossler**[3], **Achim Gossler**[3], **Andrew P. McMahon**[2], and **Raphael Kopan**[1]

[1]*Department of Molecular Biology and Pharmacology and Department of Medicine at Washington University School of Medicine, 660 South Euclid Avenue, Campus Box 8103, St. Louis, MO 63110*

[2]*Department of Molecular and Cellular Biology, Harvard University, 16 Divinity Ave, Cambridge MA 02138*

[3]*Institute for Molecular Biology OE5250, Medizinische Hochschule Hannover, Carl-Neuberg-Str. 1 D-30625 Hannover, Germany*

Summary

The Notch pathway regulates cell fate determination in numerous developmental processes. Here we report that Notch2 acts non-redundantly to control the processes of nephron segmentation through an RBP-J dependent process. Notch1 and Notch2 are detected in the early renal vesicle (RV). Genetic analysis reveals that only Notch2 is required for the differentiation of proximal nephron structures (podocytes and proximal convoluted tubules (PCT)) despite the presence of activated Notch1 in the nuclei of putative proximal progenitors. The inability of endogenous Notch1 to compensate for Notch2 deficiency may reflect sub-threshold Notch1 levels in the nucleus. In line with this view, forced expression of a γ-secretase independent form of Notch1 intracellular domain drives the specification of proximal fates where all endogenous, ligand-dependent Notch signaling is blocked by a γ-secretase inhibitor. These results establish distinct (non-redundant), instructive roles for Notch receptors in nephron segmentation.

Keywords

Notch; RBPjk; Wnt4; proximal tubule; podocytes; nephron segmentation

Introduction

The kidney is an essential excretory organ that maintains osmotic, acid-base and electrolyte equilibrium. The critical importance of the kidney makes it a common target of systemic diseases, developmental syndromes and drug toxicity. The functional unit of the mammalian kidney is the nephron; each nephron patterns along a proximal-distal axis into distinct functional domains; proximal to distal there are the glomerulus, proximal tubule, loop of Henle and distal tubule. How this critical regional structure is established is not well understood.

Nephrons form from a simple epithelial precursor, the renal vesicle (RV) itself a product of a Wnt-induced mesenchymal to epithelial transition in the outer cortex (Carroll et al., 2005). The RV begins a series of molecular changes reflected by a stereotyped set of morphological and molecular changes. Morphologically, the RV transitions through a comma, then an S shaped body stage before fusing with the adjacent epithelium of the ureteric bud-derived collecting duct system to establish a continuous tubular network. Asymmetric expression of Brn-1 (Nakai et al., 2003), E-cadherin and cadherin-6 (Cho et al., 1998a) provide some of the first evidence for polarization of the proximo-distal axis (the future glomerulo-collecting duct axis) but it is not until the S-shaped body stage that the future proximal-distal axis is readily distinguishable.

At this time, Pax-2 is highly expressed within the distal portion of the S-shaped body, including the region that fuses to the ureteric bud. Podocyte precursors, which differentiate into glomerular podocytes, reside in the proximal limb of the S-shaped body (the visceral epithelial cells) and express high levels of Wilms' tumor-1 (WT-1; (Kreidberg et al., 1993)). Adjacent to the podocyte in the cleft of the proximal limb the vascular endothelial network of the future glomerular filtration apparatus starts to assemble. Though fate-mapping studies have not addressed the contribution of distinct regions within the S-shaped body to the future nephron, a cadherin-6 positive domain that lies between the presumptive podocytes and the Pax2(+) distal tubule progenitors is likely to give rise, at least in part, to the proximal convoluted tubule, a *Lotus tetragonolobus* lectin (LTL; (Laitinen et al., 1987)) binding epithelium in the mature nephron first visible at E14.5-15.5 in the mouse. The process of nephron formation continues at the periphery of the mouse kidney up to postnatal day 7; newborn kidneys thus contain nephrons at all stages of development.

Prior work examining the expression of Notch pathway components (Chen and Al-Awqati, 2005; Leimeister et al., 2003; Piscione et al., 2004) and modulating Notch signaling (Cheng et al., 2003; Wang et al., 2003) argued for a Notch pathway activity in mammalian nephrogenesis. *Notch* genes encode single-transmembrane receptors that mediate short-range communication between cells. Receptor binding to ligand expressed on adjacent cells triggers the shedding of its extracellular domain and the subsequent cleavage of the transmembrane domain by the enzyme γ-secretase (for review, see (Mumm and Kopan, 2000)). On γ-Secretase mediated proteolysis, the Notch intracellular domain (NICD) is released and translocates to the nucleus where it associates with a DNA-bound REL-like protein (CBF1/RBPjk in vertebrates) and promotes transcription of its targets (Fryer et al., 2004; Lubman et al., 2004). In mammals, four Notch homologues (*Notch1* through *4*) and at least 5 ligands [Jagged1 (Jag1), Jag2, Delta-like (Dll) 1, Dll3 and Dll4] mediate these signaling events.

Notch1, Notch2, Dll1 and Jagged1 mRNA are detected in the RV and its derivative; the expression domain of *Notch1* partially overlaps with *Notch2* in the S-shaped body (Chen and Al-Awqati, 2005). Notch2 and Jagged1 are also expressed in the collecting duct. Humans haploinsufficient for Jagged1 (Li et al., 1997) are prone to Alagille syndrome, one symptom of which can result in the development of renal abnormalities (McCright, 2003; Piccoli and Spinner, 2001) whereas abnormal glomerulogenesis is observed when Notch2 activity is reduced (McCright et al., 2001). *Notch3* expression has been reported in the distal portion of the S-shaped body (Piscione et al., 2004), however, a lacZ knockin into the Notch3 locus indicates that only the glomerulus and blood vessels may express Notch3 (HTC and RK, unpublished observations).

To date, no specific study has addressed the regional specific action of the Notch pathway in nephron patterning though the general, organ wide inhibition of γ-secretase activity suggested that Notch activity is likely to be important as podocytes and proximal tubules are lost when γ-secretase activity is abolished (Cheng et al., 2003; Wang et al., 2003). However, the observed phenotypes cannot be unequivocally attributed to loss of Notch signaling due to the existence of multiple other substrates of γ-secretase.

Here we have addressed the specific function of *Notch1* and *Notch2* by tissue-specific modulation of their activity. These studies reveal distinct roles for *Notch1* and *Notch2* in nephron development. Notch2 activity is essential for patterning of the proximal regions of the nephron, while *Notch1* is normally activated, and when over-activated is capable of proximalizing the nephron, it is not sufficient for the development of proximal cell fates. Thus, local activation of Notch2 during renal tubule morphogenesis is a central determinant of segmented pattern in the mammalian nephron.

Materials and Methods

Notch2, RBPSUH (RBP-J) and Notch1 mutant animals

We crossed *Pax3-cre*^{tg/+};*N2*^{f/+} (*floxed Notch2*)/+ males (Engleka et al., 2005) to *N2*^{f/f} females to obtain *Pax3-cre*^{tg/+}; *N2*^{f/f} embryos or pups. We crossed *Pax2-cre*^{tg/+}; *N1*^{Δ1/+} (heterozygote for a null allele, (Conlon et al., 1995)) males to *N1*^{f/f} females to produce *Pax2-cre*^{tg/+}; *N1*^{f/Δ1} embryos. *Pax2-cre*^{tg/+};*RBP-j*^{f/+} (Ohyama and Groves, 2004; Tanigaki et al., 2002) males were crossed with *RBP-J*^{f/f} females to produce *Pax2-cre*^{tg/+}; *RBP-J*^{f/f} embryos. Using the same scheme, we also generated *Pax2-cre*^{tg/+}; *N2*^{f/f} pups which had the same phenotype as *Pax3-cre*^{tg/+}; *N2*^{f/f} *pups*. In some cases, we analyzed *Pax2-cre*^{tg/+}; *N1*^{f/Δ1}; *Dll-1*^{lacZ} embryos (Hrabe de Angelis et al., 1997).

Six2-GFP::Cre males were crossed to *Rosa*^{Notch} (Notch1 intracellular domain, (Murtaugh et al., 2003)) females to obtain *Rosa*^{Notch}/+; *Six2-GFP::Cre*^{tg/+} embryos. All mice used in this study were maintained on mixed backgrounds. Embryos were genotyped by standard PCR protocol. Noon of the day on which a vaginal plug was scored was designated as embryonic (E) day 0.5. The day when pups were born was designated as their first postnatal day (P1).

Generation of Notch1-/- ←→ Wild type chimeric embryos

The procedure is described in detail in Hadland et al (2005). Briefly, compound heterozygotes for the Rosa26 locus and N1^{Δ1} were crossed, blastocysts removed and cultured. LacZ-expressing control and Notch1-deficient ES cells were derived from Rosa26/+ and *N*^{Δ1/Δ1}; Rosa26/+ embryos, respectively. ES cells with normal karyotype were then injected into E3.5 wild type CD1 blastocysts, which were then transferred into the uterus of pseudopregnant CD1females. Whole-mount β-gal (described below) was done on the kidneys harvested from embryos at E16.5, before paraffin-embedded sectioning.

Metanephric organ culture

Mouse metanephric organ culture was performed as described by Rogers et al (1991). Briefly, kidneys were removed from E12.5 mouse embryos and cultured on transwell filters (Falcon, pore size 1 μm) at an air-fluid interface in a serum-free medium consisting of equal volumes of Dulbecco's modified Eagle medium and Ham's F12 medium containing 25 mM Hepes, sodium bicarbonate (1.1 mg/mL), 10 nM $Na_2SeO_3.5H_2O$, 10^{-11} M prostaglandin E1, and iron-saturated transferrin (5 μg/mL). Medium was refreshed every day and the metanephroi were cultured for as long as 6 days.

Histology and immunohistochemistry

The kidneys or the cultured explants were fixed in Bouin's fixative or in 4% paraformaldehyde (for LTL and BrdU analysis), embedded in paraffin and sectioned at 5 μm. The sections were then stained with hematoxylin and eosin for histological analysis. For immunohistochemistry, the sections were boiled in Trilogy (Cell Marque) for antigen retrieval. Dilution of the antibodies and the lectins was as follows: rabbit anti-mouse cadherin-6 (1:300; kindly provided by Dr. Dressler; (Cho et al., 1998a), CK8 (TROMA1; 1:10; Developmental Studies Hybridoma Bank), E-cadherin (1:1000; Transduction Labs), Jagged 1 (1:200; Santa Cruz), N-CAM (1:300, Sigma), Pax-2 (1:200; Covance), WT-1 (1:100, Santa Cruz), synaptopodin (1:40, gift from Dr. P. Mundel), laminin a1 and FITC-conjugated LTL (1:100; Vector Labs). Hoechst (0.5 μg/mL, Sigma) was used for nuclear staining. Fluorescein- and Cy3-conjugated anti-IgG corresponding to the species of the primary antibodies was used to visualize the antigen. For cadherin-6, E-cadherin and Jagged1, we used horseradish peroxidase (HRP)-conjugated IgG followed by tyramide-conjugated FITC or Cy3 for better results. For Notch1 detection, metanephroi were fixed in Bouin's fixative after 6 days in organ culture, dehydrated and

embedded in paraffin wax. 7μm sections were boiled in Trilogy for antigen retrieval, pre-blocked with PBS supplemented with 1% BSA, 0.2% skim milk, and 0.3% Triton X-100. A rabbit primary Notch 1 antibody (1:200, abcam ab27526) was used, followed by a biotinylated anti-rabbit IgG (1:3000). The Vectastain ABC kit (Vector Laboratory, Inc) and tyramide-conjugated Cy3 (TSA-Plus Cyanine 3, PerkinElmer, 1:100) were used to detect the signal.

To detect cleaved Notch1 in metanephroi, the following modified method was used. After incubation of the primary antibody V1744 (1:500, Cell Signaling Technology, a division of New England Biolabs), the sections were treated with horseradish peroxidase (HRP)-conjugated anti-rabbit IgG (1:1000; Jackson ImmunoResearch), tyramide-conjugated FITC (NEN, PerkinElmer; 1:1000), and then HRP-conjugated anti-fluorescein antibody. The antigen was then visualized with tyramide-conjugated Cy3 (Cy3 Plus, NEN; 1:400).

Detection of Lim1 was done with anti-Lim1 antibody (Chemicon International, (Karavanov et al., 1996)) with slight modification to the manufacturer's protocol. The kidney was fixed in MEMFA (MOPS 0.1M pH7.4, EGTA 2mM, MgSO4 1mM, formaldehyde 3.7%) for one hour before embedding in paraffin. Rehydrated sections were boiled in Trilogy (Cell Marque) for antigen retrieval, and incubated with anti-Lim1 antibody at 5ng/mL (1:200 of stock). To visualize the antigen, it is necessary to apply horseradish peroxidase (HRP)-conjugated anti-rabbit IgG followed by tyramide-conjugated Cy3. This allows double staining with other primary rabbit antibodies like anti Pax2.

For whole mount staining, metanephroi were fixed in 4% paraformaldehyde, washed in PBS, and incubated in the blocking solution (MABT:100mM maleic acid pH 7.5, 150mM NaCl, 0.1% Tween-20; plus 2% Blocking Reagent; Boehringer Mannheim) for one hour before adding anti-CK8antibody (1:10) for overnight incubation at room temperature. After extensive wash in MABT, the specimen was incubated with the Cy3-conjugated anti-rat IgG (1:1000). After this step, the metanephroi were incubated with FITC-LTL (1:200) for one hour at room temperature, and then washed by PBS.

β-galactosidase (β-gal) staining to detect LacZ activity

The kidneys were fixed in 4% paraformaldehyde for 2 hours before whole-mount β-gal staining at room temperature overnight. The specimens were embedded in paraffin, sectioned, and stained with antibody, and/or counterstained with diluted hematoxylin or Nuclear Fast Red (Vector Laboratories). After incubation with the primary antibody or FITC-conjugated LTL, the sections were treated with HRP-conjugated IgG or anti-FITC antibody followed by color development using diaminobenzidine as substrate.

Quantification of BrdU-labeling cells

BrdU (5-Bromo-2′-deoxyuridine) solution containing 5-Fluoro-2′-deoxyuridine (10% of the BrdU concentration) was injected intraperitoneally in pregnant mice 2 to 3 hours prior to kidney harvest. The samples were prepared and sectioned as described above before incubated with mouse anti-mouse BrdU antibody (1:200) (Becton and Dickinson). It was visualized by Cy3 plus following HRP-conjugated IgG incubation. The sections were then subjected to staining with another antibody (Jagged1 or Pax2), and then Hoechst nuclear stain. The single-color images were merged into one RGB file magnified in Adobe Photoshop. For BrdU-labeled Pax2 cells, we counted the number of BrdU-stained Pax2-expression cells and the number of Pax2-expressing cells within the Pax2-expressing renal vesicles/early nephrons from one wild type and one mutant kidney (19 renal vesicles/early nephrons from each sample. Each sample containsmultiple sections). The data were presented as percentage of BrdU-positive Pax2 cells within the Pax2-expressing cells. For BrdU labeling index of Jagged1 cells, sections from three different wild type and three different mutant kidneys were included and 15 Jagged1 clusters

were counted in each kidney sample. Within each cluster we counted the number of BrdU-stained Jagged1-expressing cells and the number of Jagged1-expressing cells; and calculated the percentage of BrdU-labeled Jagged1 cells in the Jagged1-expressing cells. Student t-test was used in the first comparison, and one-way ANOVA in the second comparison. $p<0.01$ was considered statistically significant.

In situ hybridization

Briefly, kidney samples were fixed in 4% paraformaldehyde (PFA) in PBS for 24 hours at 4C and processed for OCT embedding. Frozen blocks were sectioned at 16um thickness and air dried. Slides were post-fixed in 4% PFA for 10min, followed by three PBS washes, 3min each. Slides were treated with Proteinase K, acetylated and rinsed and dehydrated prior top use. Digoxigenin labeled riboprobes were made and column purified according to manufacturers instructions (Roche Applied Science). Hybridization was performed in a humidified chamber with a 200 μl probe and a parafilm coverslip at 68°C overnight. After hybridization, non-specific signal was removed by SSC washes and RNaseA digestions (detailed protocol is available upon request). Slides were then washed in MBST (100 mM Maleic acid, 150 mM NaCl, 0.1% tween20, pH to 7.5) and blocked with 5% HISS (heat in-activated sheep serum) in 2%BMB (Roche Applied Science) in MBST, before adding anti-Digoxigenin-AP antibody (1:4000 dilution) in 1%HISS, 2%BMB in MBST and incubated overnight in a humidified chamber at 4C. Following extensive washes, signal was developed using BM Purple (BM) for 1 to 6 days in a humidified chamber at room temperature.

Results

Conditional deletion of *Notch2* in the kidney causes complete loss of glomeruli and proximal tubules

To investigate the *in vivo* function of Notch receptors during nephrogenesis, we employed a Cre-mediated knockout strategy to disrupt these genes in the kidney mesenchyme using the *Pax3-cre* line (Li et al., 2000), which induces recombination in the metanephric mesenchyme (Grieshammer et al., 2005; Perantoni et al., 2005). Kidneys from $Pax3\text{-}cre^{tg/+}$; $Rosa26R^{tg/+}$ embryos (Soriano, 1999) display LacZ expression in all metanephric mesenchyme-derived tissues, including comma- and S-shaped body and stromal tissue, while the ureteric bud derivatives remain unlabeled. The early and broad recombinase activity assures an early and complete recombination of alleles that is specific to the mesenchymal compartment and their epithelial derivatives (Fig. S1A, B; see also (Grieshammer et al., 2005; Perantoni et al., 2005)).

Viable, normal $Pax3\text{-}cre^{tg/+}$; $N2^{f/f}$ newborns were obtained at Mendelian ratios (data not shown). However, despite feeding successfully (data not shown), $Pax3\text{-}cre^{tg/+}$; $N2^{f/f}$ animals died 24 to 48 hours after birth. Gross anatomical examination revealed that $Pax3\text{-}cre^{tg/+}$; $N2^{f/f}$ had smaller kidneys than $Pax3\text{-}cre^{tg/+}$; $N2^{f/+}$ siblings (Fig. 1A-D) and a small bladder suggested failure to produce urine (black arrows, Fig. 1A,C). During postnatal day 2 (P2), Notch2 deficient kidneys appeared to have lost vascular integrity (Fig. 1D). We observed hemorrhage into the interstitial spaces in $Pax3\text{-}cre^{tg/+}$; $N2^{f/f}$ P1 kidney (Fig. 1G, circle). The renal pelvis was collapsed, the papilla was flattened (Fig. S2A,B) and the collecting ducts (turquoise arrow, Fig. 1E-H) were less extensively branched than those of wild type or heterozygote $Pax3\text{-}cre^{tg/+}$; $N2^{f/+}$ littermates, even though $N2^{f/f}$ remains intact in the collecting duct network of the mutant. The nephrogenic zone, where the nephron initiating mesenchymal-to-epithelial transition takes place, appeared similar in thickness in both heterozygote and mutant kidneys (blue arrows, Fig. 1E,G), indicating a normal progression of the epithelialization process. In contrast, S-shape bodies (yellow arrows), convoluted renal epithelia (green arrows) and glomeruli (red arrows), were not histologically distinguishable

(Fig. 1E-H). Thus, the cause of death was renal failure due to the absence of a filtration apparatus. Heterozygote kidneys were indistinguishable from wild type in their morphological and histological features; hence we used "wild type" throughout to encompass both genotypes, although the exact genotype is detailed in the figures.

To address the state of nephrogenesis, we used immunohistochemical methods to examine the residual renal tubules that were present in the mutant kidneys (green arrowheads in Fig. 1G,H and Fig. S2E). Epithelial ductal labeling with anti Cytokeratin 8 (CK8) antibodies (specific for ureteric bud-derivatives; (Hemmi and Mori, 1991)) confirmed that a branched collecting duct was present as expected (Fig. 2C,E). Expression of WT-1, a zinc-finger-containing transcription factor, expressed at low levels in the MM and at high levels in podocytes progenitors from the S-shaped body stage (Fig. 2A), was only detected in the MM surrounding the tips of the UB (Fig. 2B). Furthermore, while LTL, a marker specific for mature proximal convoluted tubules (PCT), labeled numerous tubules in the wild type at E16.5 (Fig. 2D), no LTL-positive structures were detectable in the mutants (Fig. 2C). Thus, the organization of proximal fates was clearly compromised by Notch2 removal. In contrast, a comprehensive analysis of E-cadherin and CK8 indicated that distal nephrons were Notch2-independent. Both RV-derived epithelia and collecting duct epithelium express E-cadherin, whereas CK8 is only expressed in the collecting ducts. Many E-cadherin positive, CK8-negative tubular structures were detected in mutant kidneys. Several of these were continuous with the ureteric bud tips (Fig. 2E,E'). Whereas proximal tubules also express E-cadherin, the lack of LTL-binding activity, the continuity with the duct, their smaller size and the regular-shaped lumen (see Fig. 1H and S2E) indicate that renal tubules formed in the absence of Notch2 and most likely comprise only distal tubule segments of the nephron. Together, these data suggest that Notch2 is essential for the establishment of proximal podocyte and proximal convoluted tubule cell fates during nephron segmentation.

Notch2-deficient renal vesicles initiate the segmentation process but fail to establish the proximal fates

To examine the early patterning of RV-derivatives that preceded establishment of mature fates, we analyzed expression of a number of key reporters of these events. In both wild type and mutant kidneys, a mesenchymal Pax2 domain forms around the UB tip (Fig. 3A,B and data not shown). $Pax2^{High}$ mesenchymal cells were congregated around the tips of the UB (compare with WT-1 staining in Fig. 2B). Neural cell adhesion molecule (N-CAM) is expressed in the mesenchymal cells and in their derivatives, including the nascent renal vesicle. In wild type, N-CAM-positive cell clusters with elevated Pax2 expression appeared adjacent to the UB tip (Fig. 3A). In Notch2 mutants, we detected similar groups of amorphic $Pax2^{High}$, N-CAM-positive, CK8-negative structures located close to the UB tips (Fig. 3B,E). These clusters were positive for two signature processes of epithelialization: cellular polarization, indicated by formation of a laminin α1-positive basal lamina deposition ((Abrahamson et al., 1989), Fig. 3C,D)), and the synthesis of epithelial adhesion molecules (E-cadherin, Fig. 3E). Therefore, a robust mesenchymal condensation and MET occurs normally in Notch2-deficient metanephric mesenchyme.

The analysis of E-cadherin expression revealed three types of epithelial structures in the Notch2 mutant kidneys. First, the aforementioned early renal vesicles: small cell clusters located just below the tips of the UB that expressed $Pax2^{High}$ (#1 in Fig. 3E); the second, larger epithelial clusters of Pax2 positive, E-cadherin positive cells (#2 in Fig. 3E), a structure potentially analogous to comma- or S-shaped bodies or a "transitional" structure between the early renal vesicle; and a third structure that was tubular in shape, $Pax2^{low}$ and E-cadherin positive (#3 in Fig. 3E).

We examined the expression of WT-1, Cadherin 6 and E-cadherin for any evidence of putative podocyte/proximal tubule precursors in the Notch2-deficient renal epithelia. As was the case with LTL, Cadherin-6, an adhesion molecule thought to be expressed in the precursors of proximal convoluted tubules in S-shaped bodies, was not detected in Notch2-deficient kidneys (Fig. 4A,B). Further, WT-1^{High} podocyte precursors were also absent (Fig. 4A',B'). On close examination, the data suggested that proximal segmentation initiated, but failed to establish independent proximal identities. During early stages of nephrogenesis preceding formation of the S-shaped body, Pax-2 is expressed in all epithelia and is required to initiate expression of WT-1 (Dehbi et al., 1996); up-regulation of WT-1 inhibits Pax2 expression (Dehbi et al., 1996; Ryan et al., 1995). As in the wild type (Fig. 4A',A''), we observed WT-1 expression in Notch2 deficient nephrons that appeared to segregate from Pax2, such that cells containing lower levels of WT-1 displayed relatively higher levels of Pax2 and vice versa (Fig. 4B',B''; 4A''',B'''). Further evidence of polarity comes from analysis of Lim1; Lim1 expression is restricted to cells within the RV that are closest to the ureteric bud tip (Fig. 4C) and this is observed in Notch2 mutant kidney (Fig. 4D). Thus, the initiation of RV polarity appears to be Notch2-independent, but the establishment of stable regional identities in distinct proximal and distal regions of the developing nephron is defective and proximal fates are absent from the S-shaped body.

To address Notch pathway activation in normal nephron segmentation, we analyzed the spatial and temporal expression domain of Notch pathway proteins, in conjunction segment-specific markers. Jagged-1 protein was first detected in clusters of Pax2^{Low} expressing epithelial cells in early renal vesicles (Fig. 4E). In the absence of a good antibody to Delta-like 1 (Dll-1), we monitored the presence of LacZ knocked into the *Dll-1* gene in *Dll-1^{LacZ}* heterozygotes (Hrabe de Angelis et al., 1997). *Dll-1^{LacZ}* was also present in a subset of renal vesicle cells (Fig. 4G) that also contained activated Notch1 (Fig. 4H,I) and Lim1 (Fig. 4C). Jagged1 expression and N1-ICD accumulation became elevated on morphogenesis of the RV to the S-shaped body (Fig. 3G,I,J,4C,G). Although the cell fates have not been mapped to date, these observations suggest that activated Notch1, Jagged1 and Dll-1^{LacZ} expression are likely to mark more proximal precursor populations within renal vesicles and their early derivatives and are thus among the first markers of segmentation. Distal precursors within the S-shaped body expressed E-cadherin, high levels of Pax2 (Pax2^{High}; (Ryan et al., 1995)) but no Jagged1/N1-ICD (Fig. 3F,H,I). Podocyte precursors were WT-1 positive, Pax2^{Low} and Jagged1 negative; some contained N1-ICD (Fig. 3J,4F,I,Supplemental Fig. 3C). In the S-shaped body, *Dll-1^{LacZ}* expression overlapped with, but was broader than, the *Jagged1* domain in most S-shaped bodies. Whether this reflects real differences or the possible perdurance of ß-galactosidase activity is unclear. Dll1^{LacZ} was detected in a few E-cadherin-expressing distal precursors and in some podocyte precursors (Figure S4D). In this respect, the *Dll-1^{LacZ}* expression domain resembled the pattern of Notch1 activation better than the Jagged1 domain (Fig. S4C, D). We suggest that Jagged1-positive, *Dll-1^{LacZ}* expressing, N1-ICD containing, Pax2^{Low} cells most likely define proximal regional fates and Jagged1 is likely a better marker of proximal convoluted tubule precursors than *Dll-1* (the functional significance of *Dll-1* is discussed below). Unfortunately, while a detailed in situ expression analysis has been published for Notch receptors (Chen and Al-Awqati, 2005;Leimeister et al., 2003;Piscione et al., 2004), the absence of a suitable antibody has prevented mapping of Notch2 protein distribution.

We next addressed whether the Jagged1-expressing proximal region precursors within the renal vesicle and early RV derivatives the first to down regulate Pax2 (Fig. 3F,G) contain N1-ICD in Notch2-deficient kidneys. A small group of Jagged1-expressing cells were detected in virtually every Notch2-deficient early epithelial cluster (Fig. 4F,I), consistent with the possibility that initiation of proximal patterning is initially independent of Notch2. N1-ICD was detectable in these Jagged1-expressing cells (Fig. 4I inset) indicating that Notch1 signaling was apparently active in these cells. Clearly, Notch1 activity could not compensate for the loss

of Notch2 in subsequent patterning steps. This observation leaves open the possibility that Notch1 may contribute to the establishment of the earliest polarity pathway. Note that Pax2 expression in Jagged1-positive, Notch2-deficient cell clusters in the RV derivatives remained ubiquitous and high, consistent with impairment in acquisition of proximal and podocyte fates.

In conclusion, segregation of WT-1, Pax2 and Lim1 expression initiated and was accompanied by transient acquisition of a proximal precursor fate (Jagged1 positive, N1-ICD present). However, podocyte precursors (WT-1^{High}) never formed. This is because Notch2-deficient epithelial cells could not resolve proximal from distal fates, as evident from the simultaneous expression of markers typical for proximal and distal differentiation at the S-shape stage. Notch2 deficient cells either die or adopt a Notch2-independent distal fate. We thus conclude that the transitional epithelial structures marked as #2 in Figure 3E represent defective comma- or S-shaped bodies where segmentation has initiated but the specification of appropriate regional identities has failed.

Notch2-deficient proximal precursors have reduced capacity to proliferate

Three hypotheses can explain why morphologically distinct comma- and S-shaped bodies fail to form in the Notch2-deficient kidneys. First, cells with dual identity (i.e. expressing both Jagged1 and Pax2) die, resulting in failure to form comma- and S-shaped bodies. Second, due to global proliferation defects in the early renal epithelia, abnormal epithelial structure forms. Third, Jagged1-positive, proximal tubule precursors are unable to expand and, in their absence, typical S-shaped bodies fail to form.

The first possibility was addressed by examining the distribution of active caspase3, an early marker of apoptosis; no significantly enhanced apoptosis was observed (data not shown). The second explanation was addressed by pulse-labeling S-phase cells with BrdU and the fraction of Pax2^{High} cell examined in renal epithelia close to the ureteric bud tips; we observed a BrdU positive fraction of ~50% in both wild type and *Notch2* mutant metanephroi (54% vs 48%, *p*>0.1, Fig. 5). Thus, a general proliferative defect does not underlie abnormal tubule morphogenesis in Notch2 mutants. When proliferation was scored specifically in Jagged1-expressing cells, the subpopulation of *Notch2*-deficient, Pax2^{High}, *Jagged1*-expressing cells entered the cell cycle two fold less frequently than their wild type counterparts ($F_{(6, 15)}= 8.697$, *p*<0.001; Fig. 5). Therefore, Notch2 activity is required for normal proliferation of proximal regional precursors.

Notch1 is not required for cell fate determination during early nephron formation

To test if Notch2 was sufficient on its own for nephron segmentation in the absence of any Notch1 input, we generated *Pax3-cre$^{tg/+}$*; *N1$^{f/f}$* embryos. However, these failed to survive beyond E9.5 (data not shown) and consequently were uninformative. Two alternative strategies were adopted. First, we used chimera analysis with ES cells deficient for Notch1 (Fig. 6). Second, we used *Pax2-cre* transgenic mice (Fig. 7; (Ohyama and Groves, 2004)).

We examined chimeric kidneys generated by injecting *N1$^{\Delta1/\Delta1}$*; *Rosa26-lacZ$^{tg/+}$* embryonic stem cells (ES cells; described in (Hadland et al., 2004; Nichols et al., 2004)) into wild type blastocysts. *N1$^{\Delta1}$* contains a large deletion of the locus (Conlon et al., 1995)). We analyzed 7 chimeric mice with *Rosa26$^{tg/+}$*, *N1$^{\Delta1/\Delta1}$* cells and 4 with matched *Rosa26$^{tg/+}$* wild type controls. In all, lacZ positive cells contributed extensively to normal-looking renal vesicles, S-shaped bodies, and elongating nephrons, consistent with the absence of an early function for Notch1 (Fig. 6B). Many glomeruli were composed entirely from *Notch1*-deficient podocytes. The number of *N1$^{\Delta1}$* podocytes that surrounded a wild-type capillary tuft were within the normal range (Fig. 6F). Further, the contribution of the *Notch1*-deficient cells to the LTL$^+$ proximal convoluted tubules was also extensive (Fig. 6D,D'). Thus, there is no cell-autonomous

requirement for Notch1 activity to establish proximal renal tubule fates; however, we could not rule out a non-autonomous contribution from Notch1-expressing cells intermingled with N1-/- cells.

To determine whether any requirement for Notch1 exists, a *Pax2-cre*^{tg} transgene was used to remove Notch1 function from the metanephric kidney. Cre-mediated recombination is catalyzed in the condensing metanephric mesenchyme and in ureteric bud-derivatives (supplemental Figure S3A-B; (Ohyama and Groves, 2004)). Compound heterozygotes *Pax2-cre*^{tg}; *N1*$^{f/\Delta 1}$ embryos were normal at embryonic day 12.5 but died at E13.5 from unrelated vascular failure and hemorrhage in the internal organs (data not shown). We therefore removed the E12.5 metanephroi from *Pax2-cre*$^{tg/+}$; *N1*$^{f/\Delta 1}$ embryos and littermate controls (some of which also carried the *Dll1*^{lacZ} allele) and examined their development.

Notch1 protein is detected in the plasma membranes of duct and renal epithelial cells (inset in Fig. 7C, supplemental Figure S3E-F). Intense apical staining indicates accumulation of Notch1 in S-shaped bodies (inset in Fig. 7C and supplemental Figure S3E-F). Staining for Notch1 protein confirmed it was absent in duct and renal epithelia of *Pax2-cre* containing metanephroi (inset in Fig. 7D, supplemental Figure S3 G-L). Accordingly, no accumulation of N1-ICD was detected in renal epithelia of *Pax2-cre*$^{tg/+}$; *N1*$^{f/\Delta 1}$ embryos (supplemental Figure S3C-D). In contrast to Notch2, Notch1 deficient metanephroi appeared morphologically and histologically normal; they contained LTL-positive proximal tubules (Fig. 7B), E-cadherin positive/CK8 negative distal tubules (not shown), and WT-1^{High}, synaptopodin-positive (Mundel et al., 1997) podocytes (Fig. 6D). In contrast, *Pax2-cre*$^{tg/+}$; *N2*$^{f/f}$ embryos developed kidneys lacking proximal tubule and podocytes (data not shown), indicating that *Pax2-cre*$^{tg/+}$ used in this study removes Notch alleles before the critical window described previously (Cheng et al., 2003). Thus, Notch1 is not required for regional organization of distinct cell fates.

RBPjk deletion mimics the effect of Notch2 deficiency on nephron formation

One possible explanation for the critical role of Notch2 and the failure of active Notch1 signaling to normally complement Notch2's action would be that Notch2 has acquired a unique, RBPjk-independent activity. To address this issue, we generated *Pax2-cre*$^{tg/+}$; *RBP-J*$^{f/f}$ mice (Tanigaki et al., 2002). *Pax2-Cre*$^{tg/+}$;*RBP-J*$^{f/f}$ embryos were normal at embryonic day 12.5 but died at E13.5; when cultured at E12.5, metanephroi from *Pax2-cre*$^{tg/+}$; *RBP-J*$^{f/f}$ embryos branched properly, but failed to produce LTL-positive proximal convoluted tubules or WT-1^{High} podocytes (Fig. 7E-H). Thus, Notch2 most likely acts in a conventional, RBP-J-dependent pathway during nephron segmentation.

Notch1 can stimulate proximal fates and inhibit distal ones when ectopically activated in nephron precursors

A second possible explanation for the failure of Notch1 signaling to compensate for Notch2 could be a requirement for distinct levels of signaling inputs; the existence of activation thresholds for the Notch targets Hes1 and Hes5 was recently demonstrated in organ culture (Ong et al., 2006). If so, higher amounts of N1-ICD may be able to compensate for Notch2 in activating its targets and promoting formation of proximal pattern.

To test this hypothesis, we used a metanephric mesenchyme-specific line *Six2-GFP::Cre*. This Cre strain will be described more fully elsewhere. Importantly, *Six2-GFP::Cre* is active in the cap stage, slightly later than the *Pax2-cre* but before RV formation (Xu et al., 2003). Hence, a stable recombination results in a genetic modification of the MM and its derivatives. To elevate N1-ICD levels, we created *Rosa*^{Notch}/+; *Six2-GFP::Cre*$^{tg/+}$ mice. In these animals *Six2-GFP::Cre* excises a "stop" cassette and constitutive expression of N1-ICD activates Notch1 signaling (Murtaugh et al., 2003). Pups with this genotype were born in the correct Mendelian

ratio but displayed severely hypoplastic kidneys (Fig. 8A) where the UB underwent a single branching event (Fig. 8B). The absence of Six2-producing cells at E13.5 in the $Rosa^{Notch}/+$; $Six2\text{-}GFP{::}Cre^{tg/+}$ kidney suggested that lack of branching was secondary to the loss of GDNF-producing MM cells (data not shown).

Despite the branching deficit, multiple tubular epithelial structures formed from the WT-1; Pax2 positive cell clusters (Figure 8Ba-c). These tubular epithelia expressed both LTL (Fig. 8Bb, 8C) and Slc34a1 (not shown), characteristic of proximal convoluted tubules. To determine whether activated Notch1 accelerated the formation of proximal tubules, E11.5 metanephroi were cultured for 4 days. At this stage, there were very few LTL-positive tubules present in wild-type; however, metanephroi that overexpressed N1-ICD had already developed numerous LTL-positive tubules (Fig. 8C,C'). Furthermore, the activity of N1-ICD was independent of Notch2 since LTL-positive proximal convoluted tubules appeared even in the presence of DAPT (Fig. 9). In summary, N1-ICD can direct development of proximal nephron fates that are normally controlled by Notch2, consistent with a model in which N1-ICD is present at sub-threshold levels during normal nephron patterning.

Discussion

Notch2 maintains or induces proximal fates in the developing nephron

Mesenchymal cells in the metanephric blastema form renal epithelia in response to factors secreted by the UB tips (Carroll et al., 2005). The first epithelial structure (early renal vesicle stage) lacks distinctive morphological features, although the expression patterns of genes such as *Brn-1* (Nakai et al., 2003) suggest that polarization starts soon after epithelialization. Within the asymmetrical comma- and S-shaped body, molecular markers of the three main epithelial lineages (distal tubules, proximal tubules and podocytes) map to discrete epithelial domains. This process of renal epithelial segmentation may still require "classical", UB derived inductive function as mesenchyme induced for a shorter time only gives rise to distal tubule fates while the formation of morphologically distinct proximal tubules and podocytes from MM requires at least 24 hr exposure to the inducer (Saxen, 1987). Moreover, the ability of Pax-2 to induce WT-1, and the ability of WT-1 to inhibit Pax-2 (Ryan et al., 1995), should be enough to support segregation of the podocyte lineage from the distal tubule, but is not sufficient to account for formation of proximal convoluted tubules.

Recently, it was demonstrated that segmentation required γ-secretase activity (Cheng et al., 2003; Wang et al., 2003), an enzyme with many substrates including Notch receptors (Kopan and Ilagan, 2004). Moreover, the sensitivity of renal epithelia to γ-secretase inhibitors is informative: distal tubules are resistant to the drug while proximal tubules and podocyte are sensitive to it. Once S-shaped bodies form, they are no longer sensitive to the inhibitor (Cheng et al., 2003). This observation suggested that a γ-secretase dependent process acts to establish podocyte and proximal tubule identities in RV derivatives. In this report, we identify Notch2 as the first key determinant involved in acquisition of proximal fates in the nephron.

The idea that Notch signaling may provide this function is supported by marker analysis. Until recently, only a few markers distinguish the segments within the S-shaped body: WT-1 marks podocyte precursors (Kreidberg et al., 1993), Cadherin-6 likely proximal tubule precursors, and E-cadherin and Brn-1 more distal tubule precursors (Cho et al., 1998b; Nakai et al., 2003). The usefulness of Pax2 as a segmentation marker is underappreciated; differential expression distinguishes prospective distal and Bowman's capsule precursors from proximal precursors and podocytes (here and (Ryan et al., 1995)). Examination of all these markers, Notch ligands and Notch1 activation suggests that segmentation initiates within the renal vesicle or its earliest derivative. Here, a small subset of cells acquires proximal precursor markers (Jagged1, activated Notch1); expression may be activated at the boundary of Lim1

positive and negative territories. N1-ICD and Jagged1 may provide the earliest markers for proximal tubule precursors; we anticipate that this population expands and expresses Cadherin-6, and develops into mature proximal tubules that are LTL$^+$.

Our studies indicate that activated N1-ICD, Lim1 and Jagged1 are all observed in the RV of Notch2 deficient newborn mice; thus, it is likely that segmentation initiates independently of Notch2. However, persistent expression of the distal tubule marker (Pax2^{High}) suggests a function for Notch in Pax2 inhibition, while the reduced proliferation rates of Jagged1 expressing cells suggest Notch2 promotes the proliferative expansion of this progenitor domain. Asymmetrical expression of *Dll-1^{LacZ}* in the renal vesicle is another early indicator of RV segmentation (Fig. 4G). Kobayashi et al (2005) have shown that Lim1-deficient kidneys produce lower *Dll-1* and arrest at the renal vesicle stage. Part of the Lim1 phenotype may be explained by failure to activate *Dll-1* and hence Notch2 at this stage. Indeed, hypomorphic *Dll-1* allele (Kiernan et al., 2005) results in reduction of proximal tubule formation (Fig. S4). These observations suggest that Lim1 can serve as an upstream regulator of Notch ligands and thus, Notch signaling. However, Lim1-/- ES cells do not contribute to the regions of the comma- and S-shaped bodies indicating that Dll1 expressing, wild type cells cannot rescue Lim1-deficient cells. Lim-1 is thus required also during proximalization. The early RV distribution of Lim1 was maintained in the Notch2-deficient RV (Fig. 4D), but in the more advanced nephron, Lim1 expression assumed an abnormal pattern: although they will all eventually adopt the distal fate, cells accumulating at the proximal end expressed high Lim1 (Fig. 4C). Therefore, the separation of the distal and proximal lineages and the differentiation of proximal tubule and podocyte precursors require two parallel inputs, one provided by Notch2 and another from Lim1.

Notch1 and Notch2 have non-overlapping activities

We demonstrate here that while direct activation of Notch1 is observed in proximal precursors of the S-shaped body, removal of Notch1 activity with *Pax2-Cre* had no impact on the establishment of proximal fates. Thus, Notch1 is clearly non-essential for this process and Notch2 is the only γ-secretase substrate that plays a significant role in these patterning events. As soon as Notch was identified as an X-linked locus in Drosophila (Welshons, 1958), it was realized that the wing phenotype associated with Notch mutations was due to haploinsufficiency. Notch1 is haploinsufficient in vertebrates as well: Myelination in the mouse is slowed in Notch1 heterozygote animals (Givogri et al., 2002), and human tri-cuspid heart valve development and maintenance of valve flexibility throughout adult life require both alleles of Notch1 (Garg et al., 2005). Importantly, no kidney disease is reported in these kindred; however, as this manuscript underwent revisions, a human haploinsufficiency for Notch2 was reported to cause Alagille syndrome (McDaniell et al., 2006). This would not be possible if Notch1 and Notch2 played redundant roles in human nephron development; we infer from this data that in human, as in the mouse, Notch2 is the dominant receptor during nephron segmentation.

While Notch1 and Notch2 differ in their ability to activate targets (Ong et al., 2006), they have the same affinity to RBP-J (Lubman et al., 2006). Notch-responsive promoters may respond differentially to similar nuclear concentrations of activated Notch receptors within the nephron, becoming inactive if this amount falls below a threshold (Ong et al., 2006). What then can be the mechanistic basis for these findings?

The observation that N1-ICD overexpression can promote the proximal fates when endogenous Notch processing (and thus signaling) is abolished supports a model whereby sub-threshold levels of this protein in the normal renal epithelium fail to complement Notch2 deficiency. Thus, Notch1 may be a weak activator of key target(s) regulated normally by Notch2, or N1-ICD may fail to accumulate to sufficient levels in the normal kidney to functionally replace

Notch2 deficiency. Another possibility is that N1-ICD is modified in a manner that decreases its odds of association with RBP-J. This will be predicted to prevent its degradation (Fryer et al., 2004), and ironically, facilitate its detection by immunohistochemistry. When over expressed, some N1-ICD may escape modification, bind and activate critical targets.

If differences existed between N1-ICD and N2-ICD that affected binding to RBPjk or to other putative partners, where would they map within the intracellular domain? Domain swaps indicated that the divergent 426 amino acids that lie downstream of the ANK domain are not important: mice expressing a Notch2 hybrid containing this Notch1 domain (and thus deficient in the Notch2 c-terminal domain) lack a kidney phenotype (Kraman and McCright, 2005). Crystallographic analysis of the Notch1 ANK domain revealed a surface that is unique to each of the vertebrate Notch paralogs (Lubman et al., 2005). Therefore, the subtle differences in the ANK domain may be responsible for the lack of redundancy between these highly conserved receptors (see also Ong et al., 2006).

In conclusion, our study presents the first evidence for Notch2's critical role in an intrinsic patterning mechanisms that establishes proximal-distal nephron polarity. We discovered a cell type in which two different Notch molecules are present in its nucleus yet only one is critical (Notch2), a demonstration of unexpected complexity in this pathway, and provided evidence that detection of N1-ICD per se is not an unambiguous indicator of a functional role for Notch1 signaling. These results serve as an entry point to explore further details of the mechanisms controlling early nephron development. They establish that Notch2 acts to separate proximal and distal fates and in this Notch signaling most likely plays an instructive role after an initial polarizing cue (Lim1?) acts in the RV. Thus, utilization of Notch proteins in the kidney appears to be quite different from their use in the skin where all cellular identities emerge prior to and independent of Notch function (Pan et al., 2004) and where Notch1 plays a dominant role (Demehri et al, in preparation).

Supplementary Material

Refer to Web version on PubMed Central for supplementary material.

Acknowledgments

References

Abrahamson DR, Irwin MH, St John PL, Perry EW, Accavitti MA, Heck LW, Couchman JR. Selective immunoreactivities of kidney basement membranes to monoclonal antibodies against laminin: localization of the end of the long arm and the short arms to discrete microdomains. J Cell Biol 1989;109:3477–91. [PubMed: 2480964]

Carroll TJ, Park JS, Hayashi S, Majumdar A, McMahon AP. Wnt9b plays a central role in the regulation of mesenchymal to epithelial transitions underlying organogenesis of the mammalian urogenital system. Dev Cell 2005;9:283–92. [PubMed: 16054034]

Chen L, Al-Awqati Q. Segmental expression of Notch and Hairy genes in nephrogenesis. Am J Physiol Renal Physiol 2005;288:F939–52. [PubMed: 15821257]

Cheng H, Miner J, Lin M, Tansey MG, Roth KA, Kopan R. g-Secretase Activity is Dispensable for the Mesenchyme-to-Epithelium Transition but Required for Proximal Tubule Formation in Developing Mouse Kidney. Development 2003;130:5031–5041. [PubMed: 12952904]

Cho EA, Patterson LT, Brookhiser WT, Mah S, Kintner C, Dressler GR. Differential expression and function of cadherin-6 during renal epithelium development. Development 1998a;125:803–12. [PubMed: 9449663]

Cho EA, Patterson LT, Brookhiser WT, Mah S, Kintner C, Dressler GR. Differential Expression and Function Of Cadherin-6 During Renal Epithelium Development. Development 1998b;125:803–812. [PubMed: 9449663]

Conlon RA, Reaume AG, Rossant J. Notch1 is required for the coordinate segmentation of somites. Development 1995;121:1533–45. [PubMed: 7789282]

Dehbi M, Ghahremani M, Lechner M, Dressler G, Pelletier J. The paired-box transcription factor, PAX2, positively modulates expression of the Wilms' tumor suppressor gene (WT1). Oncogene 1996;13:447–53. [PubMed: 8760285]

Engleka KA, Gitler AD, Zhang M, Zhou DD, High FA, Epstein JA. Insertion of Cre into the Pax3 locus creates a new allele of Splotch and identifies unexpected Pax3 derivatives. Dev Biol 2005;280:396–406. [PubMed: 15882581]

Fryer CJ, White JB, Jones KA. Mastermind Recruits CycC:CDK8 to Phosphorylate the Notch ICD and Coordinate Activation with Turnover. Mol Cell 2004;16:509–20. [PubMed: 15546612]

Garg V, Muth AN, Ransom JF, Schluterman MK, Barnes R, King IN, Grossfeld PD, Srivastava D. Mutations in NOTCH1 cause aortic valve disease. Nature 2005;21:180–184.

Givogri MI, Costa RM, Schonmann V, Silva AJ, Campagnoni AT, Bongarzone ER. Central nervous system myelination in mice with deficient expression of Notch1 receptor. J Neurosci Res 2002;67:309–20. [PubMed: 11813235]

Grieshammer U, Cebrian C, Ilagan R, Meyers E, Herzlinger D, Martin GR. FGF8 is required for cell survival at distinct stages of nephrogenesis and for regulation of gene expression in nascent nephrons. Development. 2005

Hadland BK, Huppert SS, Kanungo J, Xue Y, Jiang R, Gridley T, Conlon RA, Cheng AM, Kopan R, Longmore GD. A requirement for Notch1 distinguishes two phases of definitive hematopoiesis during development. Blood 2004;104:3097–3105. [PubMed: 15251982]

Hemmi A, Mori Y. Immunohistochemical study of cytokeratin distribution in the collecting duct of the human kidney. Acta Pathol Jpn 1991;41:516–20. [PubMed: 1721761]

Hrabe de Angelis M, McIntyre J 2nd, Gossler A. Maintenance of somite borders in mice requires the Delta homologue DII1. Nature 1997;386:717–21. [PubMed: 9109488]

Karavanov AA, Saint-Jeannet JP, Karavanova I, Taira M, Dawid IB. The LIM homeodomain protein Lim-1 is widely expressed in neural, neural crest and mesoderm derivatives in vertebrate development. Int J Dev Biol 1996;40:453–61. [PubMed: 8793615]

Kiernan AE, Cordes R, Kopan R, Gossler A, Gridley T. The Notch ligands DLL1 and JAG2 act synergistically to regulate hair cell development in the mammalian inner ear. Development 2005;132:4353–62. [PubMed: 16141228]

Kopan R, Ilagan MXG. g-Secretase: proteasome of the membrane? Nat Rev Mol Cell Bio 2004;5:7–12.

Kraman M, McCright B. Functional conservation of Notch1 and Notch2 intracellular domains. Faseb J 2005;19:1311–3. [PubMed: 15897231]

Kreidberg JA, Sariola H, Loring JM, Maeda M, Pelletier J, Housman D, Jaenisch R. WT-1 is required for early kidney development. Cell 1993;74:679–91. [PubMed: 8395349]

Laitinen L, Virtanen I, Saxen L. Changes in the glycosylation pattern during embryonic development of mouse kidney as revealed with lectin conjugates. J Histochem Cytochem 1987;35:55–65. [PubMed: 3794309]

Leimeister C, Schumacher N, Gessler M. Expression of Notch pathway genes in the embryonic mouse metanephros suggests a role in proximal tubule development. Gene Expression Patterns 2003;3:595–598. [PubMed: 12971992]

Li J, Chen F, Epstein JA. Neural crest expression of Cre recombinase directed by the proximal Pax3 promoter in transgenic mice. Genesis 2000;26:162–4. [PubMed: 10686619]

Li LH, Krantz ID, Deng Y, Genin A, Banta AB, Collins CC, Qi M, Trask BJ, Kuo WL, Cochran J, et al. Alagille-Syndrome Is Caused By Mutations in Human Jagged1, Which Encodes a Ligand For Notch1. Nature Genetics 1997;16:243–251. [PubMed: 9207788]

Lubman OY, Ilagan MXG, Kopan R, Barrick D. Quantitative Dissection of the Notch:CSL Interaction: Insights into the Notch Transcriptional Switch. J Mol Biol. 2006in press

Lubman OY, Korolev SV, Kopan R. Anchoring notch genetics and biochemistry; structural analysis of the ankyrin domain sheds light on existing data. Mol Cell 2004;13:619–26. [PubMed: 15023333]

Lubman YO, Kopan R, Waksman G, Korolev S. The Crystal Structure of a Partial Mouse Notch-1 Ankyrin Domain: Repeats 4 Through 7 Preserve an Ankyrin Fold. Protein Sci 2005;14:1274–1251. [PubMed: 15802643]

McCright B. Notch signaling in kidney development. Curr Opin Nephrol Hypertens 2003;12:5–10. [PubMed: 12496659]

McCright B, Gao X, Shen LY, Lozier J, Lan Y, Maguire M, Herzlinger D, Weinmaster G, Jiang RL, Gridley T. Defects in development of the kidney, heart and eye vasculature in mice homozygous for a hypomorphic Notch2 mutation. Development 2001;128:491–502. [PubMed: 11171333]

McDaniell R, Warthen DM, Sanchez-Lara PA, Pai A, Krantz ID, Piccoli DA, Spinner NB. NOTCH2 mutations cause Alagille syndrome, a heterogeneous disorder of the notch signaling pathway. Am J Hum Genet 2006;79:169–73. [PubMed: 16773578]

Mumm JS, Kopan R. Notch Signaling: From the Outside In. Dev Biol 2000;228:151–165. [PubMed: 11112321]

Mundel P, Heid HW, Mundel TM, Kruger M, Reiser J, Kriz W. Synaptopodin: an actin-associated protein in telencephalic dendrites and renal podocytes. J Cell Biol 1997;139:193–204. [PubMed: 9314539]

Murtaugh LC, Stanger BZ, Kwan KM, Melton DA. Notch signaling controls multiple steps of pancreatic differentiation. Proc Natl Acad Sci U S A 2003;100:14920–5. [PubMed: 14657333]

Nakai S, Sugitani Y, Sato H, Ito S, Miura Y, Ogawa M, Nishi M, Jishage K, Minowa O, Noda T. Crucial roles of Brn1 in distal tubule formation and function in mouse kidney. Development 2003;130:4751–9. [PubMed: 12925600]

Nichols AM, Pan Y, Herreman A, Hadland BK, De Strooper B, Kopan R, Huppert S. The Notch pathway is dispensable for adipocyte specification. Genesis 2004;40:40–44. [PubMed: 15354292]

Ohyama T, Groves AK. Generation of Pax2-Cre mice by modification of a Pax2 bacterial artificial chromosome. Genesis 2004;38:195–9. [PubMed: 15083520]

Ong C, Cheng H, Chang LW, Ohtsuka T, Kageyama R, Stormo DG, Kopan R. Target selectivity of vertebrate Notch proteins: collaboration between discrete domains and CSL binding site architecture determine activation probability. J Biol Chem 2006;281:5106–5119. [PubMed: 16365048]

Pan Y, Lin M, Tian X, Cheng H, Gridley T, Shen J, Kopan R. g-Secretase functions through Notch signaling to maintain skin appendages but is not required for their patterning or initial morphogenesis. Dev Cell 2004;7:731–743. [PubMed: 15525534]

Perantoni AO, Timofeeva O, Naillat F, Richman C, Pajni-Underwood S, Wilson C, Vainio S, Dove LF, Lewandoski M. Inactivation of FGF8 in early mesoderm reveals an essential role in kidney development. Development. 2005

Piccoli DA, Spinner NB. Alagille syndrome and the Jagged1 gene [Review]. Seminars in Liver Disease 2001;21:525–534. [PubMed: 11745040]

Piscione TD, Wu MY, Quaggin SE. Expression of Hairy/Enhancer of Split genes, Hes1 and Hes5, during murine nephron morphogenesis. Gene Expr Patterns 2004;4:707–11. [PubMed: 15465493]

Ryan G, Steele-Perkins V, Morris JF, Rauscher FJ 3rd, Dressler GR. Repression of Pax-2 by WT1 during normal kidney development. Development 1995;121:867–75. [PubMed: 7720589]

Saxen, L. Organogenesis of the kidney. Cambridge University Press; Cambridge: 1987.

Soriano P. Generalized lacZ expression with the ROSA26 Cre reporter strain [letter]. Nat Genet 1999;21:70–1. [PubMed: 9916792]

Tanigaki K, Han H, Yamamoto N, Tashiro K, Ikegawa M, Kuroda K, Suzuki A, Nakano T, Honjo T. Notch-RBP-J signaling is involved in cell fate determination of marginal zone B cells. Nat Immunol 2002;3:443–50. [PubMed: 11967543]

Wang P, Pereira FA, Beasley D, Zheng H. Presenilins are required for the formation of comma- and S-shaped bodies during nephrogenesis. Development 2003;130:5019–5029. [PubMed: 12930775]

Welshons WJ. The analysis of a pseudoallelic recessive lethal system at the notch locus of Drosophila melanogaster. Cold Spring Harb Symp Quant Biol 1958;23:171–6. [PubMed: 13635554]

Xu PX, Zheng W, Huang L, Maire P, Laclef C, Silvius D. Six1 is required for the early organogenesis of mammalian kidney. Development 2003;130:3085–94. [PubMed: 12783782]
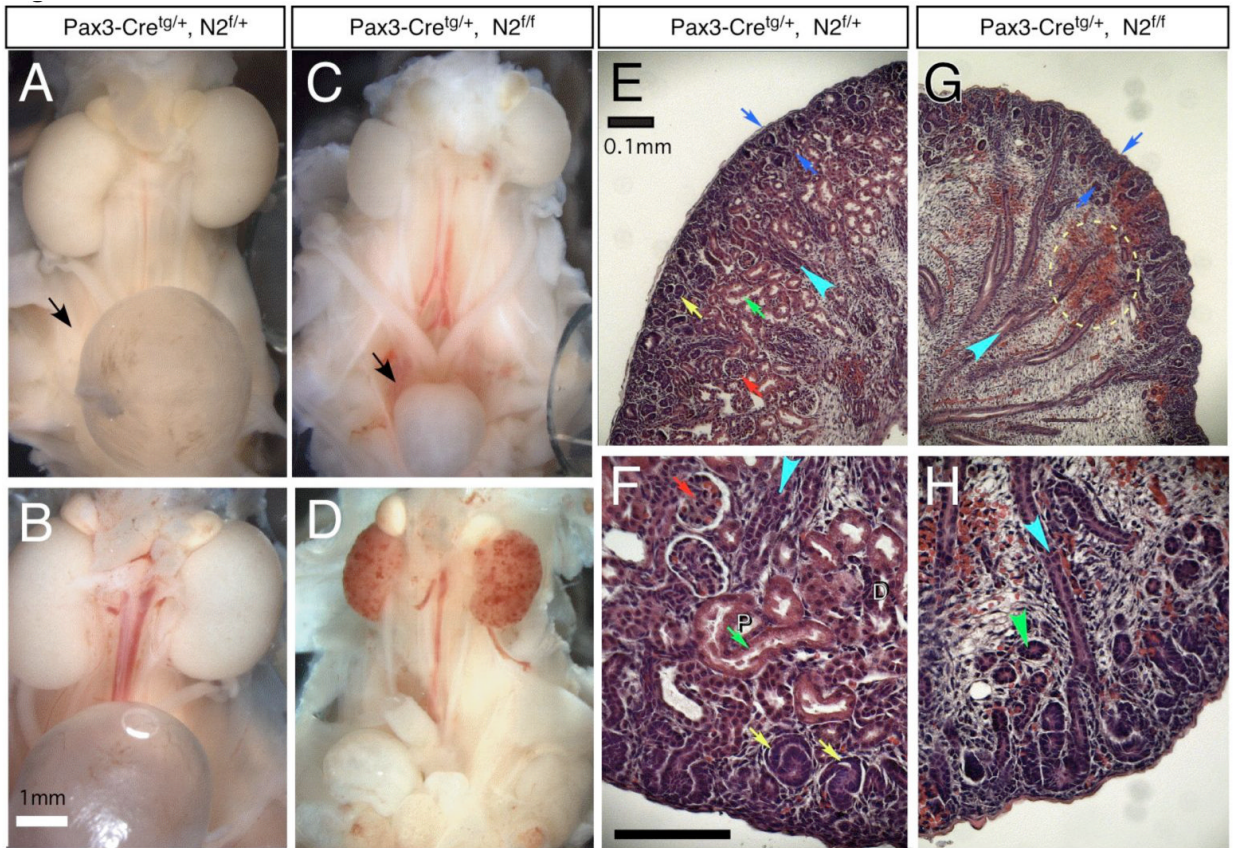
Fig. 1.
Loss of *Notch2* causes hypoplastic kidneys that do not develop glomeruli, proximal tubules
and S-shaped bodies. (A to D) The urinary system from postnatal day 1 and day 2 wild type
(A, B) or mutant (C, D) animals. Notice the size difference of the urinary bladder (arrow in A
and C). The mutant animals show spotty hemorrhage on the kidneys before they die on postnatal
day 2 (D). (E to H) Histology of day 2 kidneys from wild type (E, F) and mutant (G, H) stained
with H&E. Blue arrows flank the nephrogenic zone. Red arrow: glomerulus. Green arrow:
proximal tubule. Yellow arrow: S-shaped body. Turquoise arrowhead: collecting duct. Green
arrowhead: presumptive renal tubule in mutant. P: proximal tubule. D: distal tubule. The wild
type genotype is *Pax3-cre^{tg/+}; N2^{f/+}*; the mutant genotype is *Pax3-cretg/+; fN2/fN2*. Bar, 1mm
(A to D), 0.1mm (E to H). Red arrows mark glomeruli, green-proximal tubule (marked also
with P), turquoise- duct, yellow- S-shaped bodies, dark blue- nephrogenic zone. D indicates
distal tubules.
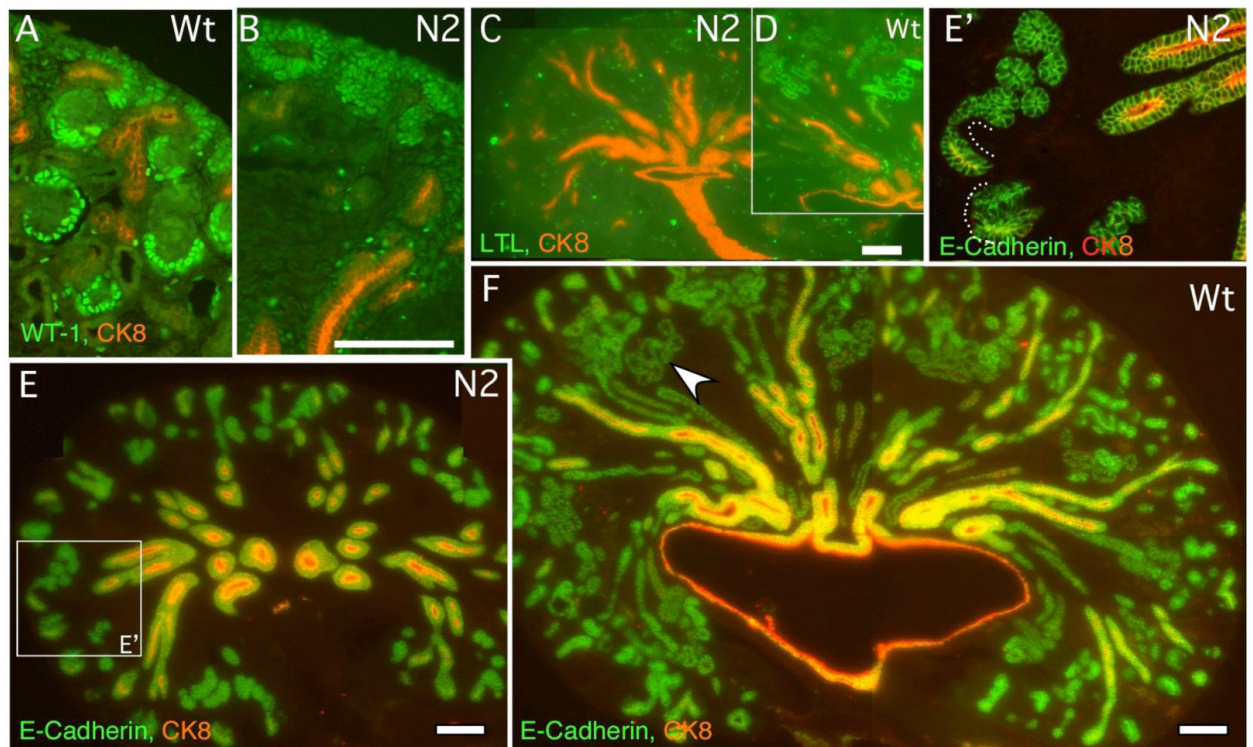
Fig. 2.
Notch2-deficient kidneys (N2) develop distal tubules without formation of podocytes and proximal tubules. (A, B) Wild type (A) kidney contains high Wilms tumor-1-expressing cells in glomerular podocytes and S-shaped bodies. The only cells that express low level of Wilms tumor-1 in mutant (B) are mesenchymal cells surrounding cytokeratin8-expressing ureteric buds (red). (C, D) No LTL-stained proximal tubules are found in mutant (C), compared to wild type (D). (E, F) Mutant kidney (E) develops numerous E-cadherin-positive, cytokeratin8-negative distal tubules, some of which are connected to cytokeratin8-positive ducts (dash line). The wild type proximal tubules, judged by morphology, also express E-cadherin (arrowhead in F). Wt: wild type. N2: Notch2 mutant. Bar, 0.1mm (A, B, E') and (C to F).
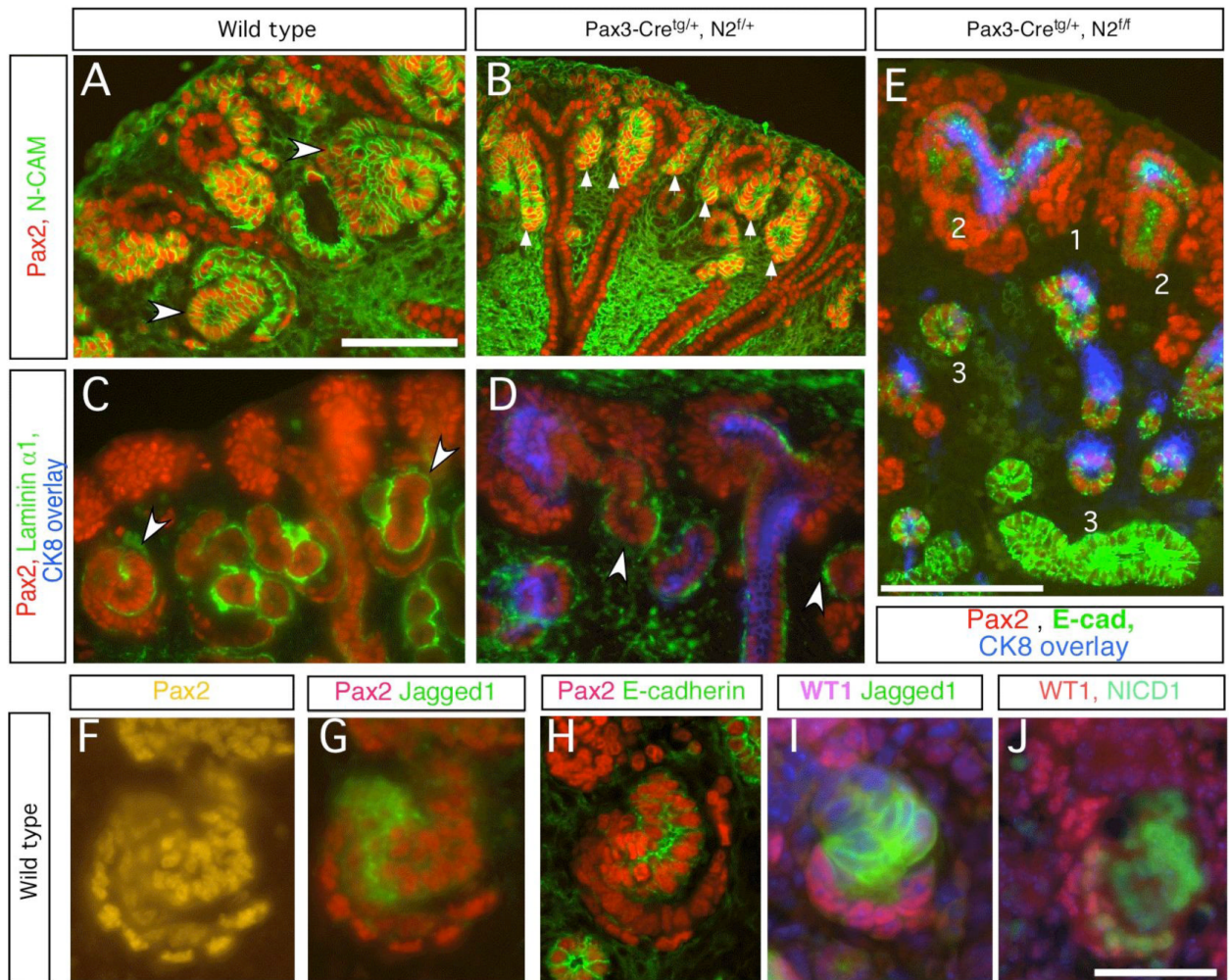
Fig. 3.
(A to E) Notch2-deficient mesenchyme undergoes normal epithelialization but the newly formed nephron fails to resolve into S-shaped body. (A, B) S-shaped bodies are seen in wild type (arrowhead in A). In Notch2 mutant, one nephron, which expresses N-CAM, can be identified at each ureteric bud tip (arrow in B). They synthesize laminin α1 (arrowhead in D), so do the S-shaped bodies (arrowhead in C). (E) Three progressive stages during nephrogenesis in the mutant are marked as 1, 2 and 3. Bar, 0.1mm. (F to J) Each of three segments in the S-shaped body expresses molecular markers (see text). Distal tubule precursors are Pax2^{high} and E-cadherin positive (F, H). Jagged1 is localized in the middle segment where proximal tubule precursors reside (G). WT-1 marks the podocyte precursors (I). N1-ICD is detectable in both the proximal and podocyte precursors (J). Bar, 0.05mm.
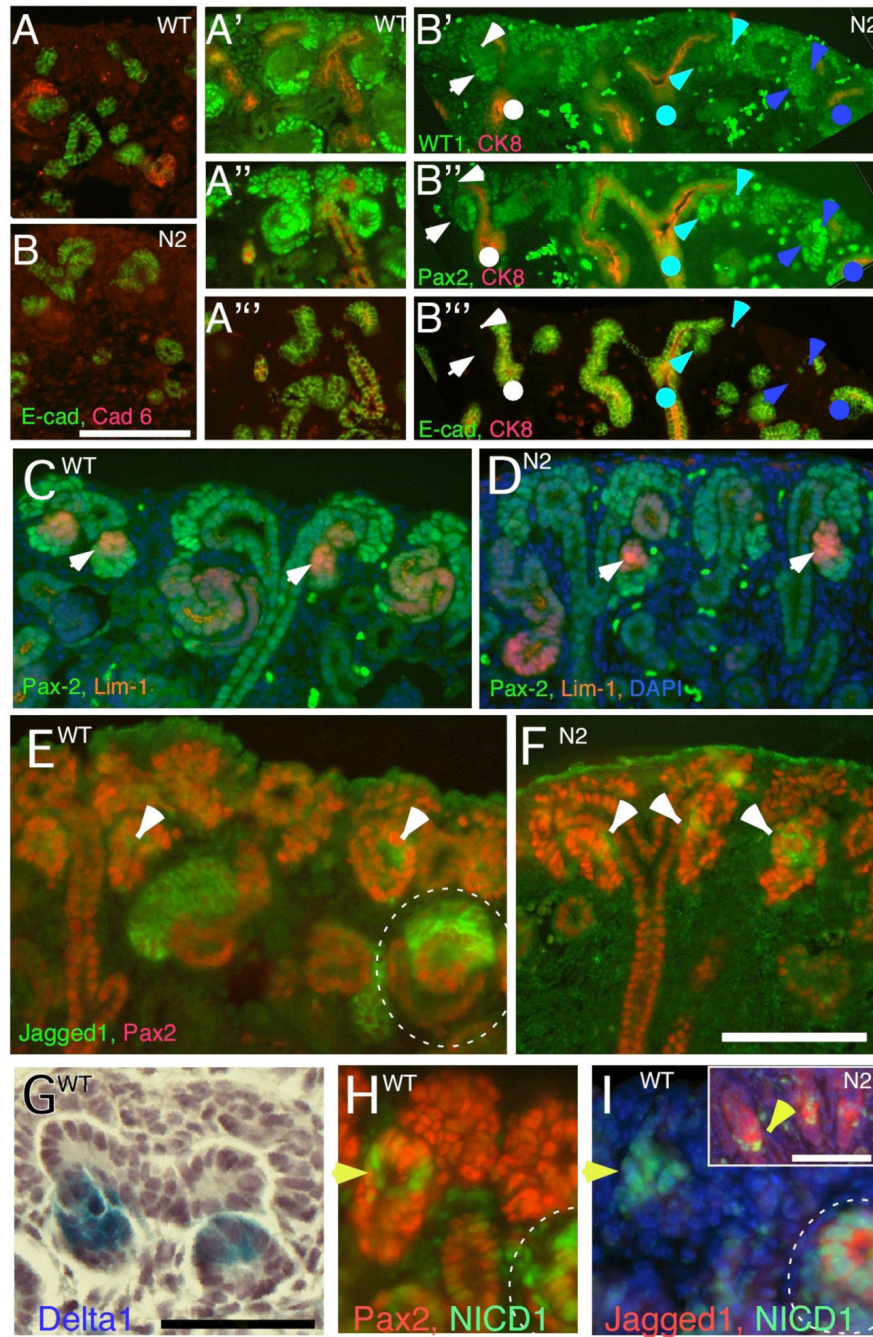
Fig. 4.
The segmentation process in Notch2-deficient nephron (N2) is impaired. (A, B) Cadherin-6-expressing cells are adjacent to E-cadherin-expressing cells in wild type (A) but no Cadherin-6-expressing cells are detectable in mutant (B). (A' through B''') Serial sections are stained with the segmentation markers Pax2, WT-1 and E-cadherin. Arrows and arrowheads indicate similar structure across all sections. (C, D) Lim1 expression pattern in the renal vesicle is similar in both wild type and Notch2 mutant kidneys (white arrow). The cells at the very proximal end of the mutant nephron express high Lim1 (D). This distribution is different from a wild type S-shaped body (C). (E) Few Jagged1-expressing cells are seen in the renal vesicle (arrowhead), and the population expends with the formation of the S-shaped body (circle). A small cluster

of Jagged1-expressing cells is seen in each of the mutant nephrons (F). *Dll-1^{LacZ}* and N1-ICD are detectable in the renal vesicle (G, H). In some cases, Jagged1 is not co-localized with N1-ICD (I). N1-ICD is still detectable in Notch2-deficient nephrons (inset in I). Bar, 0.1mm (A to F), 0.05mm (G-I).
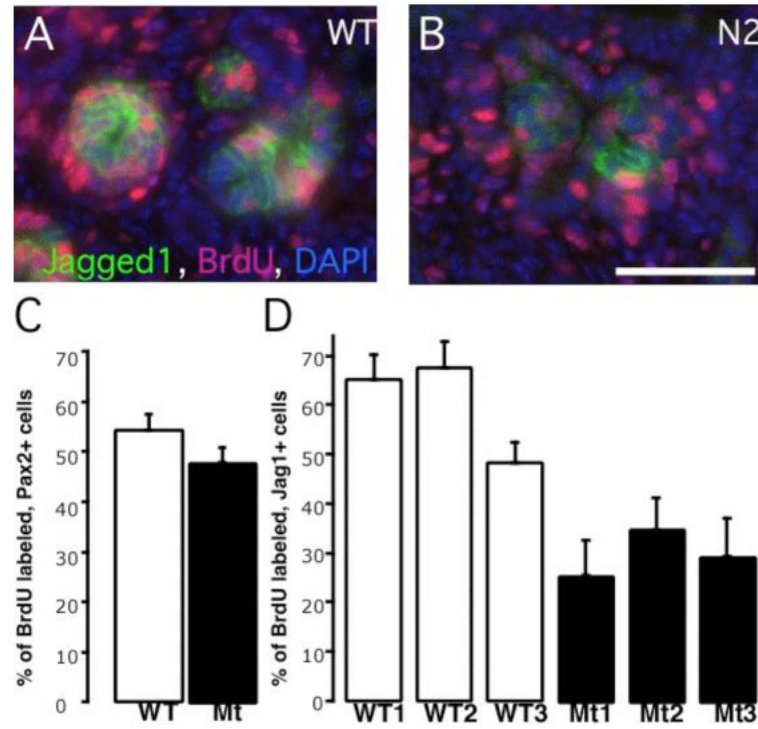
Fig. 5.
Wild type and Notch2 mutant, Pax2-expressing early renal epithelia are proliferating to a similar degree while Jagged1-expressing, Notch2-deficient clusters have few cycling cells. (A, B) Representative images of BrdU-incorporation (red) within the Jagged1-expressing clusters (green). Bar, 0.05mm. (C, D) Histogram of results from several embryos indicates the percentage of BrdU-labeled cells within the Pax2- or Jagged1 expressing domains. Data are presented as means +/- SEM (Standard error of the mean).
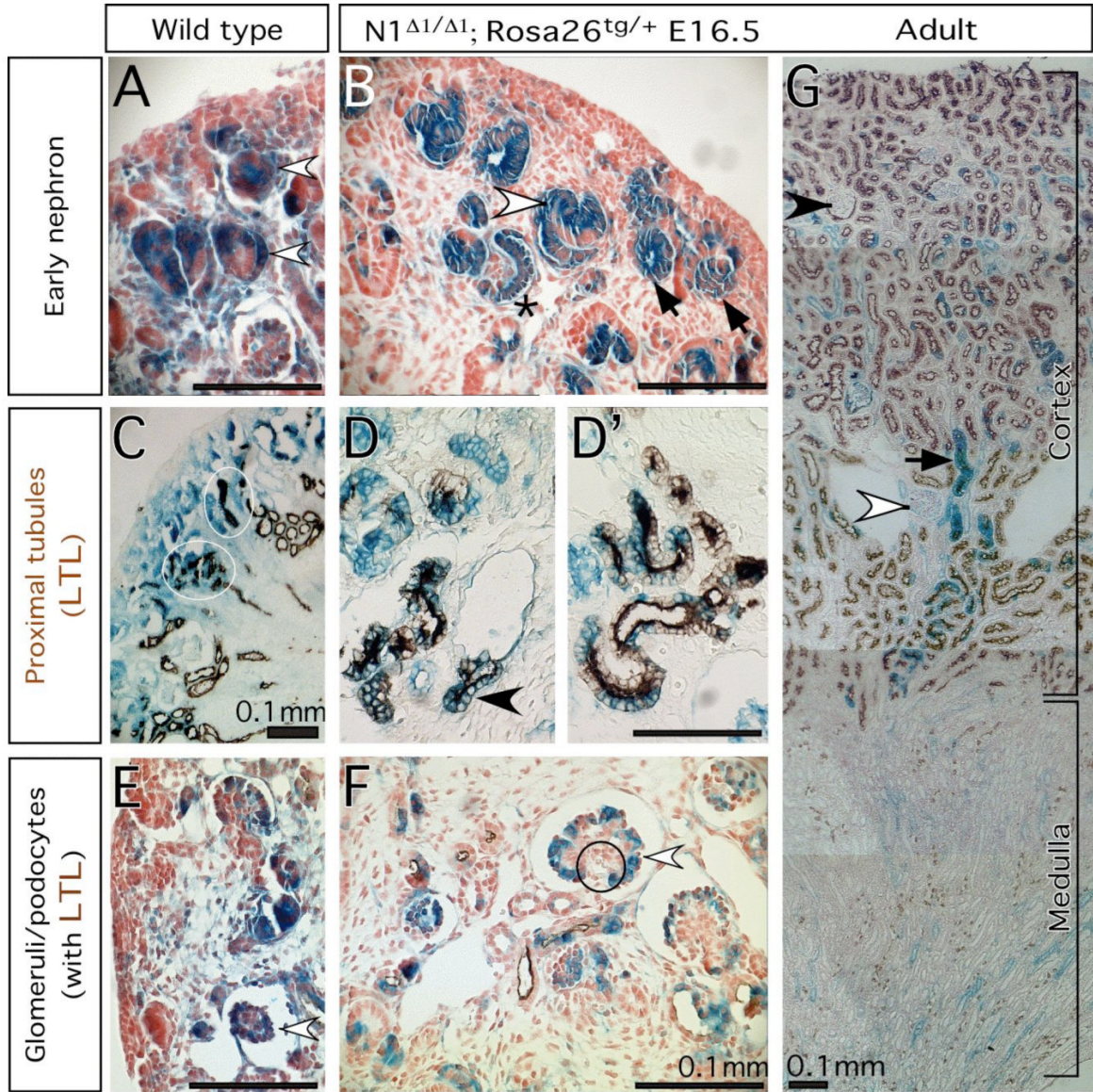
Fig. 6.
Notch1-deficient ES cells contribute to various parts of the nephron. The kidneys are harvested from E16.5 embryos (A-F) or adult (G), and subject to whole mount β-gal staining. (A, C, E) Wild type ES cells in E16.5 kidneys are found in early nephrons (blank arrowhead in A), proximal convoluted tubules (PCT, circle in C), and glomerular podocytes (blank arrowhead in E). (B, D, F, G) *Notch1-/-*; *Rosa26* ES cells contribute to renal vesicles (arrow in A), S-shaped bodies (blank arrowhead in A) and podocytes in the capillary-loop stage (star in B). (D, D') Notch1-deficient ES cells (blue) contribute to LTL-labeled PCT together with wild type cells (unstained). One LTL-labeled cross-section that composed entirely from Notch1-deficient cells is shown in D (arrowhead). (E) Glomerular podocytes develop in the absence of Notch1 (blank arrowhead). The circle indicates the capillary lumen with red blood cells in it. (G) The adult kidney is stained with LTL (brown). Some of the LTL-labeled tubules in the inner cortex are entirely derived from Notch1-/- cells (solid arrow). Blank arrowhead and sold arrowhead indicate a juxtamedullary glomerulus and a cortical glomerulus, respectively. Gray arrowhead in C, D insets mark the duct.
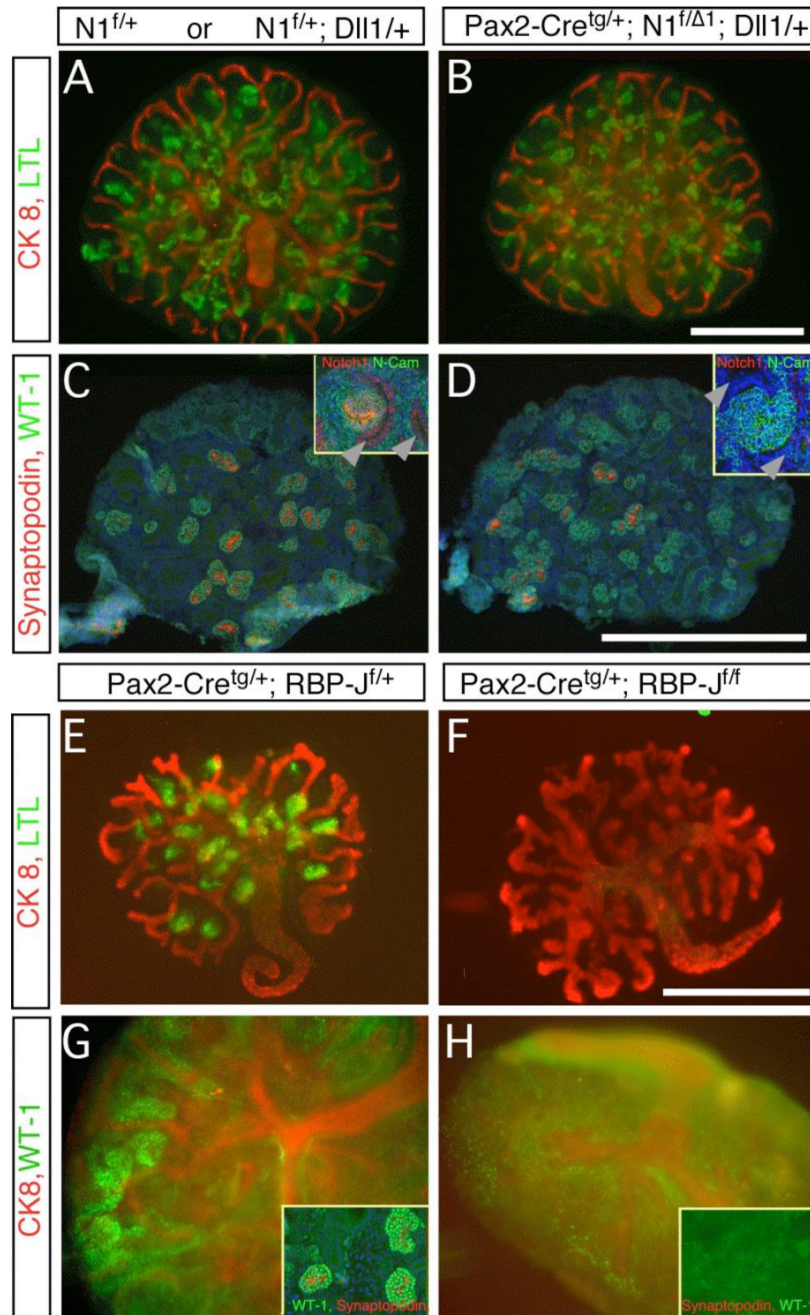
Fig. 7.
Notch1-deficient metanephroi are phenotypically wild type. The genotypes are marked above all panels. Where indicated, floxed alleles were recombined with the Pax2-Cre[tg/+] strain. (A,B,E,F) Whole mount staining of LTL (green) and CK8 (red) detects extensive renal tubulogenesis. Loss of Notch1 did not alter proximal tubule formation (D) whereas loss of RBP-J resulted in loss of LTL-positive epithelial cells. Note that loss of Notch1 or RBP-J in the duct (see Notch1 staining in inset, C-D) did not prevent duct branching. (C,D,G,H) Glomerular podocytes are labeled with WT-1 (green). In (G, H) whole mount preparation is also stained with CK8 (red). WT-1[High], synaptopodin-positive (red in C,D, inset in G) Glomeruli are present in wild type (C), Notch1 deficient metanephroi (D), and RBP-J

heterozygotes (G) but not in RBP-J deficient metanephroi (inset in H, no WT-1 or synaptopodin) (Bar, 0.5mm).
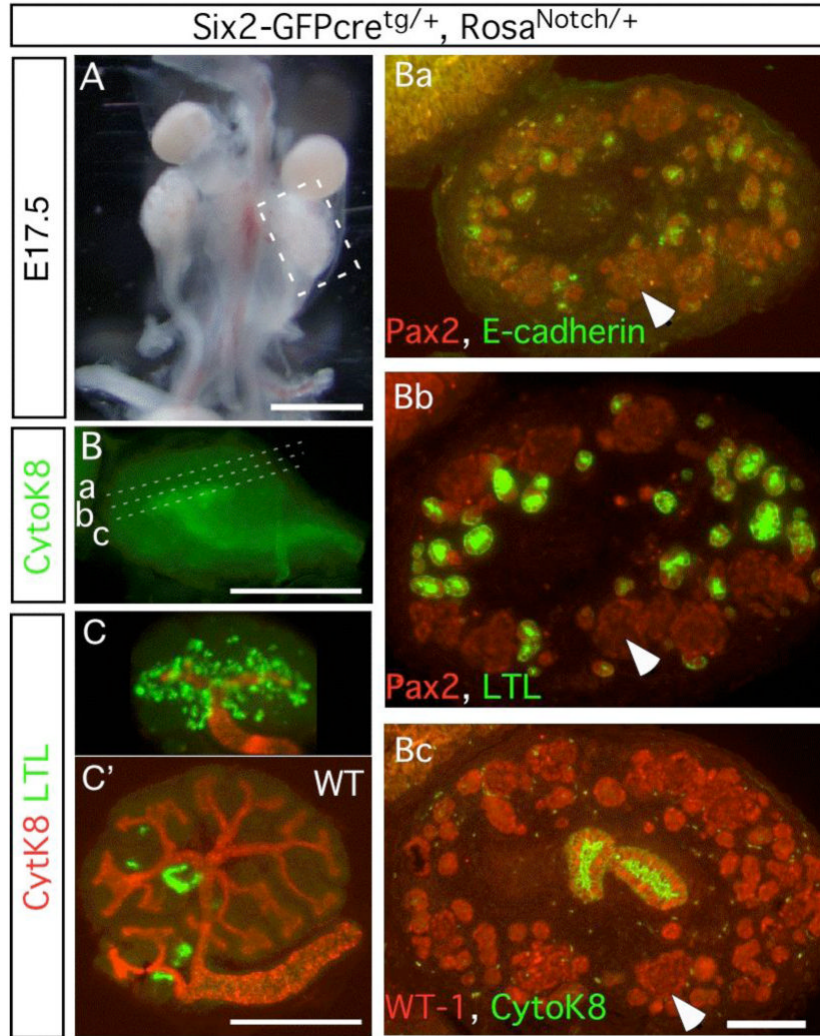
Fig. 8.
Constitutively active Notch1 promotes proximal tubule formation while inhibiting the progenitor from differentiating into podocytes and distal tubules. (A) Notch1 activation in the mesenchyme causes renal hypoplasia at E17.5. (B) The ureteric bud branches only once. Subsequent planes of sectioning are marked (a-c). CK8 is visualized using Cy3, but the image is pseudo-colored to correspond with figures Ba-Bc. (C, C') E11.5 metanephroi from mutant (C) or wild type (C') were cultured for 4 days, stained with LTL (green) and CK8 (red). (Ba-c) Serial sections of the mutant kidney are stained with markers for renal tubules. Arrows locate the same cells in adjacent sections.
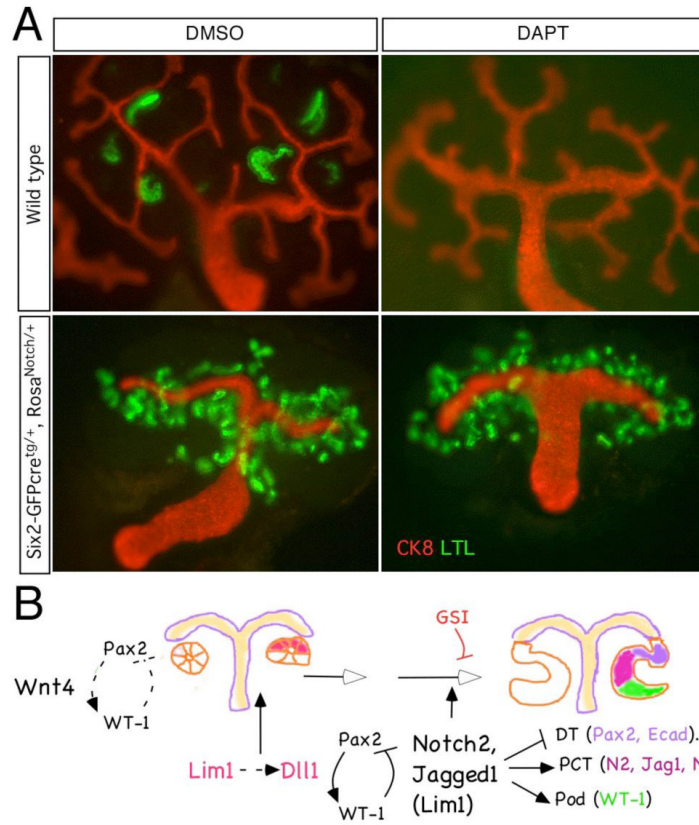
Fig. 9.
(A) Ectopic over-expression of Notch1 intracellular domain is sufficient to promote proximal tubule formation in absence of γ-secretase activity. Genotypes are shown to the left of the image; DMSO-vehicle only, DAPT- γ-secretase inhibitor. (B) A schema of the proximlization pathway. After RV induction (a Wnt dependent process) Pax2 and WT-1 begin to separate into distinct expression domains and Lim1 and Dll1 define a distal domain within the RV. However, Notch2 signals are required for separation of proximal from distal fates; in their absence (or when blocked by γ-secretase inhibitors (GSI)), only distal tubules form. See text for detail.